

GRAVITY-DRIVEN FINGERING IN UNSATURATED FRACTURES

M.J. Nicholl, R.J. Glass, and H.A. Nguyen
Geoscience Analysis Division 6315
Sandia National Laboratories
Albuquerque, NM 87185
(505)844-0945

ABSTRACT

Gravity-driven wetting-front instability is known to occur in both porous media and Hele-Shaw cells. A systematic investigative procedure for studying gravity-driven fingering in unsaturated, rough-walled fractures is described. As a first step toward understanding this system, experiments were performed in an analogue fracture consisting of two roughened glass plates held in close contact. Results from preliminary experiments in both initially dry and wet analogue fractures are presented, including measurements taken from individual fingers within a fully unstable flow field. For initially dry fractures, increasing the volume of fluid contained in the front leads to increases in both finger width and velocity. Finger velocity also was observed to increase with gravitational gradient. Once a finger structure develops in an initially dry fracture, the structure persists in subsequent infiltration events. In uniformly wet fractures, fingers are found to be more numerous and thinner and to have higher velocity than fingers formed in initially dry fractures.

INTRODUCTION

Proposed geologic isolation of high-level radioactive wastes in unsaturated fractured rock has brought to the forefront one of the most difficult technical problems in hydrogeology - unsaturated fracture flow. Development and validation of field-scale models capable of predicting flow and radionuclide transport through an unsaturated, fractured rock unit must be based on a thorough understanding of local behavior.^{1,2} Prior to Winograd's³ seminal paper expounding the potential of thick unsaturated zones in arid regions to act as a natural barrier to flow, very little theoretical or experimental research in unsaturated fractured rock had been conducted. From a theoretical viewpoint, coupling between the highly non-linear unsaturated flow equations and a variable matrix, dissected by a network of "planar" fractures with variable aperture fields, creates a very difficult problem. Likewise, the technical demands

associated with performing controlled laboratory experiments on unsaturated fractures within an unsaturated matrix has limited experimental work.

The conceptual models currently used for the performance-assessment exercises do not incorporate many small-scale processes which govern flow within unsaturated fractures.⁴ Current models assume uniform wetted structure within fractures, however, under most conditions, fractures will not develop a uniform wetted structure. Wetted-region structure in a horizontal fracture is most likely to be fractal even for a random fracture-aperture field.⁵ In non-horizontal fractures, the influence of gravity can cause infiltration flow instability and the formation of gravity-driven fingers despite the high potential gradients into the surrounding dry matrix (see Figure 1).

Instability is defined as the unconstrained growth of the inevitably occurring small perturbations characteristic of all dynamic systems. Gravity-driven wetting-front instability is manifested as the break-up of a smooth wetting front into discrete fingers oriented in the direction of the gravitational gradient (V_g). It has been shown that under certain conditions, wetting fronts exhibit gravity-driven instability in both unsaturated sands^{6,7,8,9,10} and Hele-Shaw cells, which are physical analogues for saturated flow through porous media.^{11,12,13,14,15} It is highly probable then, that gravity-driven instability also will develop in an unsaturated rough-walled fracture.

The linear stability analysis of Saffman and Taylor¹¹ assumed a constant velocity, downward displacement of one fluid (sub₂) by another (sub₁) in a vertically oriented homogeneous, isotropic Hele-Shaw cell or porous medium. Their results suggested that system stability was a function of fluid viscosity difference ($\mu_1 - \mu_2$), fluid density difference ($\rho_1 - \rho_2$), and the interfacial velocity (U). Steady planar displacement was found to be unstable at all wavelengths when the following inequality is satisfied:

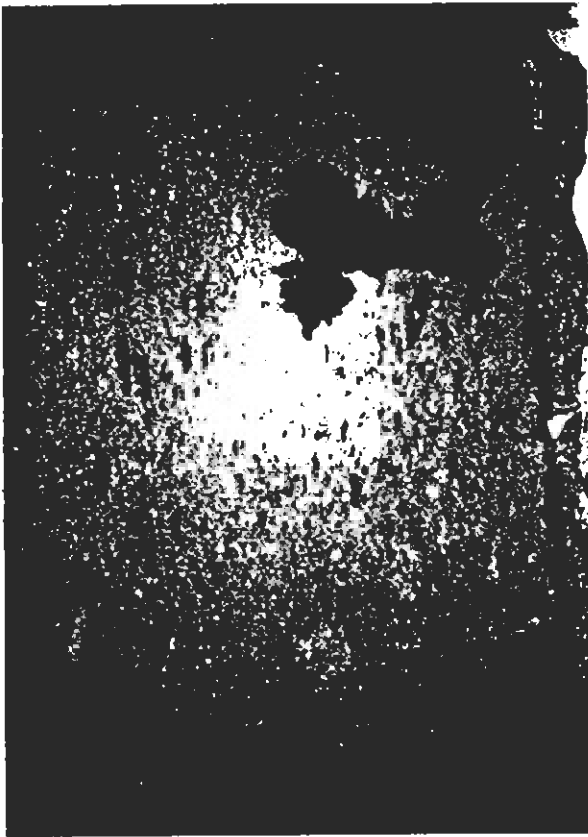


Fig. 1: Gravity-fingering and fracture/matrix interaction: Gravity-driven fingering associated with non-horizontal fractures can significantly limit the transfer of fluids and solutes between the fractures and matrix because of the reduction in wetted area within the fracture. This series of photographs shows the formation of a finger in a "half plane" fracture. A vertical fracture was simulated by securing a roughened glass plate to the face of a smooth slab of densely-welded tuff. Note that the generated flow field wets much less than 25% of the fracture plane (taken from Glass and Tidwell²).

$$kg(\rho_1 - \rho_2) - \theta U(\mu_1 - \mu_2) > 0, \quad (1)$$

where: θ - pore volume
 g - gravitational acceleration, and
 k - intrinsic permeability.

Equation 1 may be simplified for air/water systems in porous media by neglecting the density and viscosity of air with respect to those of water. The resultant inequality (Equation 2) simply states that a downward moving infiltration front will be unstable when the flux (q) through the system is less than the maximum gravitationally driven flux (q_{max}); for vertical flow, q_{max} is equal to the saturated hydraulic conductivity (K_S).

$$q < q_{max} \quad (2)$$

Chouke et al.,¹² and later Parlange and Hill¹⁶ extended Saffman and Taylor's results by incorporating the effects of capillary forces along the interface. Both approaches showed that interfacial capillary forces stabilize the front for all wavelengths below a minimum unstable wavelength. The heuristic approach taken by

Chouke et al.,¹² found this wavelength to be solely a function of fluid surface tension, while the more rigorous approach of Parlange and Hill¹⁶ also incorporated the effects of media properties. Natural and experimental systems smaller than this wavelength will not experience instability.

For instability to occur in an unsaturated rough-walled fracture, the horizontal length scale of the fracture also must exceed some minimum length (L); Equation 3 provides a first-order estimation for L in a rough-walled fracture:

$$L = \frac{2\sigma \cos\beta}{\rho g \sin\alpha a}, \quad (3)$$

where:

σ - fluid surface tension
 α - inclination from vertical
 a - mean fracture aperture, and
 β - contact angle.

The implications of wetting-front instability with regard to modeling unsaturated fracture flow are extensive. Inter-block connectivity, and

to the back side of the test-plane table. Data is acquired by a charge-coupled-device (CCD) video camera attached to the superstructure of the RTS and focused on the fracture plane. The RTS was designed such that the rigidly connected light box, test-plane table, and camera could be rotated on the support base through more than 180 degrees. This feature allows variation of V_g and rapid inversion of the test cell.

The test cell consists of two rectangular aluminum frames with 1.9 cm thick plate-glass windows. The test cell used in these experiments measures 70x39.5 cm and holds a fracture measuring 61x30.5 cm. Test fracture plates are mounted to the inside of the plate glass window, with a rubber gasket forming a pressure container between the two surfaces. Pressurization of this container on each side of the fracture removes long wavelength disturbances in the aperture field by forcing the fracture plates to be in close contact while the fracture boundaries remain open to atmospheric pressure. In the experiments described, a constant confining pressure of 20 psi was applied to each side of the analogue fracture.

All experiments were imaged and recorded at pre-determined intervals. In order to prevent image degradation, all recording and processing was done exclusively in the digital domain. The PC-based data-acquisition system utilized a DATA TRANSLATION 2862 frame grabber and the associated software. Data were acquired at 512x512 pixels, 256 grey-levels/pixel resolution using a COHU CCD. Pure de-ionized water (DI) provided insufficient contrast for the imaging system. Experimental fluid consisted of 1 g FD&C Blue #1 and 1 g FD&C Red #3 added to 1 liter of DI, producing a deep blue-purple color. Wetting properties of the experimental fluid were evaluated using capillary tubes, and found to be consistent with that of DI.

FULL FIELD INSTABILITY: INITIALLY DRY FRACTURE

By analogy to porous media and Hele-Shaw cell studies, it is expected that uniform application of fluid to an inclined, initially dry fracture at less than the maximum gravitationally driven flux (q_{max}) will result in an unstable wetting front. In preliminary trials, this boundary condition was implemented by using a porous plate and positive-displacement pump to provide a distributed source along the upper boundary of a vertical fracture. Under these conditions fingers initiated at the fracture/plate boundary, indicating a highly unstable system. Development of individual fingers appeared to be associated with local heterogeneities at the fracture/plate boundary. These local features acted as point connections between the porous plate and the fracture, providing preferential flow paths into the fracture. The abrupt onset of fingering, however, prohibited investigation of the transition from stable to unstable flow.

A second situation expected to be unstable is the redistribution of flow following the cessation of stable infiltration at q_{max} . To explore this situation, a stable infiltration front was produced by simultaneously injecting the contents of 16 evenly spaced syringes along the upper boundary of the fracture. A reservoir enclosing the fracture boundary allowed ponding of excess fluid when input rate exceeded the imbibition capacity of the fracture. This procedure yields initial/boundary conditions analogous to the surface ponding associated with a sudden precipitation event in an arid region.

Application of a finite slug allows visualization of the stable infiltration front and subsequent transition to instability. Distributing the slug through multiple point sources induces a long wave length perturbation in the advancing front (Figure 2a). Differential application of fluid allows variation in the magnitude and spatial distribution of finite perturbations to the front.

A series of slug imbibition/redistribution experiments were conducted in an initially dry fracture (see Table 2). Parameters varied during this series of full-field experiments were limited to V_g and volumetric input. Gravitational gradient was varied by positioning the RTS such that the fracture was inclined from vertical at

TABLE 2

Exp #	V_g	Vol. (cm ³)	No. of fingers	v_f (cm/min)	w_f (cm)
Initially dry fracture					
13	1.00	6.2	4	100.4	5.4
9	1.00	7.1	3	112.4	5.1
16	1.00	14.1	2	184.3	10.1
8	0.75	6.5	2	77.0	5.5
4	0.75	7.0	3	78.3	3.9
10	0.75	12.8	2	122.0	7.9
11	0.75	19.3	2	*	11.9
12	0.75	23.0	0	na	na
7	0.50	6.1	3	47.2	3.4
2	0.50	6.8	2	43.5	4.5
6	0.25	6.2	1	5.2	4.5
Initially wet fracture: persistence					
16-1	1.00	3.6	7		
13-1	1.00	5.2	3		
9-1	1.00	6.8	3		
11-2	0.75	6.5	6		
10-1	0.75	13.0	5		
11-1	0.75	19.3	2		
12-2	0.50	3.8	6		
12-1	0.50	4.0	6		
3-1	0.50	6.8	2		
Initially wet fracture: uniform field					
14	1.00	3.4	6		
15	1.00	7.5	7		

* - no measurement possible

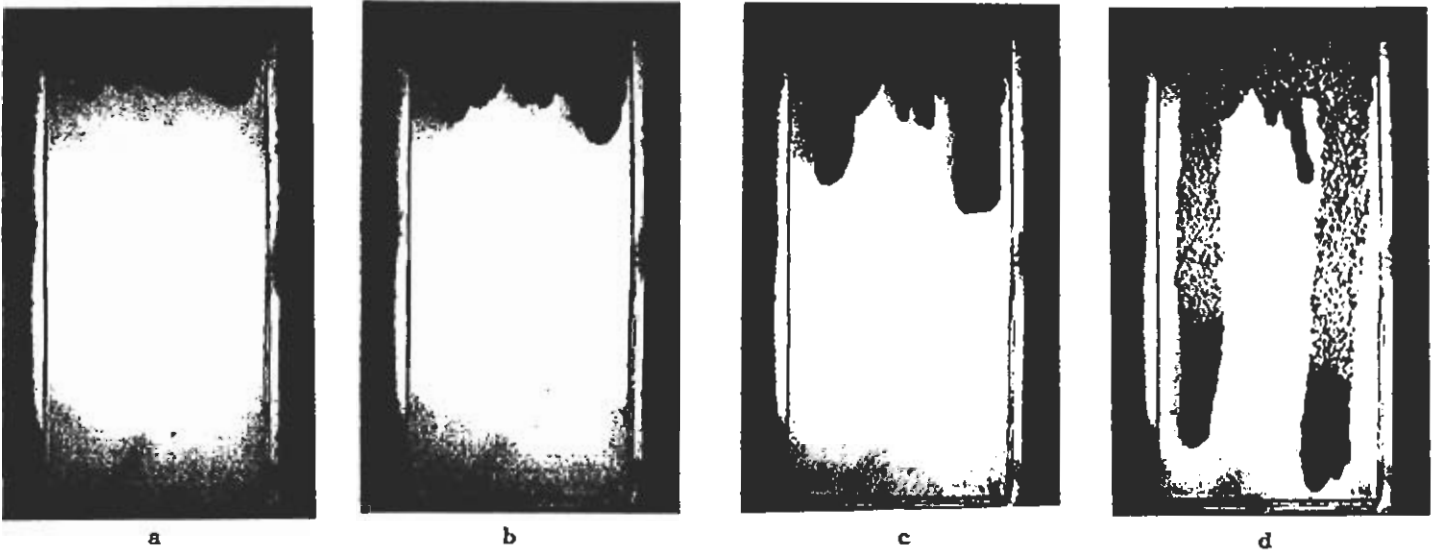


Fig. 2: Sequence illustrating the development of an unstable wetting front in an initially dry fracture (Experiment 8): a) Advancement of stable front, b) Onset of instability, c) Development of fingers, d) Fluid depletion of central finger.

angles of 0, 41.5, 60, and 75.5 degrees; corresponding to V_g of 1.0, 0.75, 0.50, and 0.25. Volumetric input to the fracture was varied over a range between 6 and 25 cm^3 . Fluid was applied with the intent of minimizing perturbations but without attempting to form a completely flat front.

Qualitative Observations

In all of the experiments conducted, fluid application produced a stable wetting front along the full width of the fracture during the initial imbibition phase. The front begins from 16 separate points that rapidly coalesce into a single front as imbibition proceeds. The resulting front is stable, but not flat (Figure 2a). The macroscopic features observed are caused by irregularities in the injection process, while smaller features result from local heterogeneities within the fracture. At any given fracture inclination, increasing the volumetric input appears to flatten the front. The dynamic effects of sustained flow at q_{max} overwhelms any irregularities in the system. This is an indication of stability, as the perturbations from uneven injection and local heterogeneity are damped out by the system dynamics.

The behavior of the wetting front changes entirely when the input slug is exhausted and imbibition ceases. The pressure gradient quickly reverses to oppose fluid advancement within the fracture. The resultant decreased flux is no longer sufficient to support a stable wetting front ($q < q_{max}$) and the onset of instability is observed (Figure 2b). The finite perturbations induced during the injection process continue to grow, forming distinct fingers. The wavelength associated with this growth is the same as, or slightly smaller than, that associated with the

stable, perturbed front.

The total potential gradient along the wetting front (V_t) is the resultant of two sets of forces; gravitational forces acting on the fluid body as a whole and capillary forces acting along the wetting and drying fronts. The water-entry pressure-head (ψ_w) acts as a driving force, pulling the wetting front forward, while air-entry pressure-head (ψ_a) along the drying front acts to restrain movement. If L_s is taken to be the saturated length of the fluid column measured parallel to V_g , then the gradient due to capillary forces (V_c) may be approximated by :

$$V_c \sim \frac{\psi_a - \psi_w}{L_s} \quad (4)$$

$$V_t = V_g + V_c \quad (5)$$

Due to the wetting properties of water in our glass fracture, the capillary gradient will be positive once the redistribution phase begins, thereby opposing the gravitational force. At the cessation of imbibition, the horizontal upper boundary of the fracture creates a relatively flat drying front (Figure 2b). Hence, the force opposing flow (V_c) is smallest at those points along the wetting front located furthest down-gradient, inducing flow to these locations. The situation is reversed during stable imbibition where $\psi_a = 0$ and V_c reinforces flow. Therefore, the downward gradient is weakest at those points furthest from the imbibition boundary and perturbations are expected to decrease in magnitude.

After the onset of instability, individual fingers rapidly develop (Figure 2c). Fingers

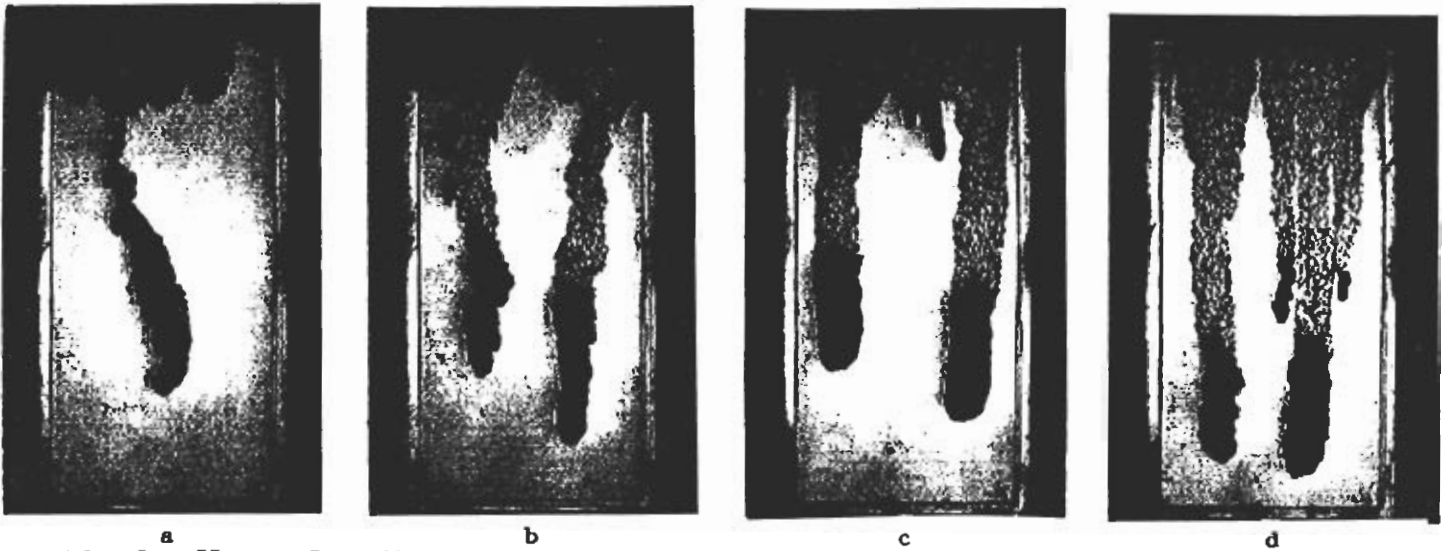


Fig. 3: Effects of gradient on unstable front development: a) Experiment 6, Image # 85, $\nabla_g = 0.25$, elapsed time = 1518 sec, b) Experiment 2, Image # 13, $\nabla_g = 0.50$, elapsed time = 104 sec, c) Experiment 8, Image # 19, $\nabla_g = 0.75$, elapsed time = 31 sec, d) Experiment 13, Image # 18, $\nabla_g = 1.00$, elapsed time = 23 sec.

consist of a coherent slug of fluid moving downward as a unit. Drainage behind the saturated tip of the finger leaves a partially saturated zone, wetted to field capacity of the fracture. Due to variation in the aperture field, saturation within the drained region exhibits a high degree of spatial variation. Fully saturated, but disconnected regions are seen as dark areas in Figure 2c. Because the tip is not replenished by flow through the drained region, it decreases in size with distance traveled. As L_s decreases within a finger, V_c increases in magnitude and the finger slows to a halt, becoming "frozen" in the fracture.

The largest and fastest fingers consume the bulk of the available fluid. As a result, less robust fingers become disconnected from the fluid source, and hence are retarded (Figure 2d). At the onset of instability the front shown in Figure 2b exhibits three growing fingers that have developed from spatial perturbations in the stable front. The center finger has the smallest L_s of the three fingers; the gradient field induces preferential flow into the outer fingers, eventually starving the center finger (Figure 2d). Widely separated fingers are more likely to fully develop than ones located close together, as there is less competition for available fluid.

Limits on volumetric input

As previously stated, volumetric input was varied in these experiments over a range of 6 to 25 cm³. The analogue fracture was not of sufficient length for fingers to fully develop at a ∇_g of 0.75 if the wetting front contained much more than 20 cm³ of fluid which is about half the total aperture volume of the analogue fracture (41.5 cm³). Current experiments are exploring input limits at the remaining ∇_g (0.25, 0.5, 1.0).

In the other limit, if one injects a sufficiently small quantity of fluid into an initially dry fracture, simple theory suggests that it will remain stationary. For the fluid to move downward, gravitational and capillary forces must be sufficient to overcome the air-entry pressure-head required for drainage at the top boundary of the fracture. Movement is expected to initiate when:

$$L_s > \frac{\psi_a - \psi_w}{\nabla_g} \quad (6)$$

Experiment 6 (Table 2, Figure 3a) appeared to be on the boundary between movement and remaining stationary. For several minutes after the cessation of imbibition the front appeared to be frozen. However, close examination revealed that the front was moving virtually pore by pore in the vicinity of maximum L_s , analogous to the process of invasion percolation.¹⁸ Approximately 24 minutes after injection a distinct tendril formed from the front, sharply increasing local gradient. The rate of pore filling was seen to increase very rapidly and the finger seen in Figure 3a developed.

Quantitative Analysis: width and velocity

Digital images were used to quantify the behavior of individual fingers after the onset of instability. Measurements were made of finger tip velocity (v_f) and finger width (w_f). Tip velocity was defined as the rate of change in position of the saturated tip in the direction of maximum gravitational gradient. Finger width was defined as the average width of the wetted domain, measured normal to the gravitational gradient over a region free from boundary effects. Preliminary data are summarized in Table 2;

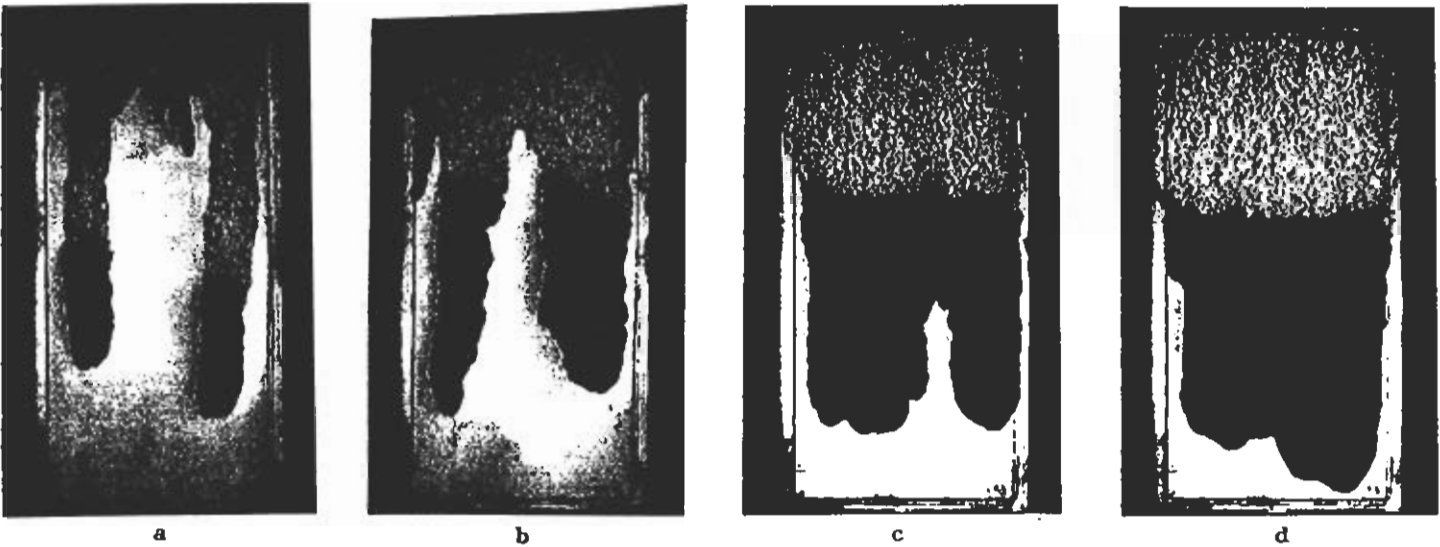


Fig. 4: Effects of volumetric input on unstable front development ($V_g = 0.75$): a) Experiment 8, Image # 19, input vol. = 6.5 cm^3 , elapsed time = 31 sec, b) Experiment 10, Image # 18, input vol. = 12.8 cm^3 , elapsed time = 23 sec, c) Experiment 11, Image # 18, input vol. = 19.3 cm^3 , elapsed time = 23 sec, d) Experiment 12, Image # 18, input vol. = 23.0 cm^3 , elapsed time = 23 sec.

finger velocity and width are given as average values of the individual fingers measured in a given experiment. Fingers were defined as distinct structural features that showed significant movement toward the bottom boundary of the fracture. At high input volumes (Experiments 11 and 12), fingers did not fully develop prior to contacting the bottom boundary of the analogue fracture, thereby limiting measurements. Digital images, illustrating the effects of V_g and volumetric input on the behavior of individual fingers, are shown as Figures 3 and 4, respectively.

The images shown in figures 3 and 4 suggest that v_f increases with both V_g and volumetric input. Raw velocity data collected from individual fingers (Figure 5) support this conjecture. Scatter within the data makes any more definite conclusions untenable at this time; it is anticipated that additional experiments will clarify the relationship between V_g , volumetric input, and velocity.

Velocity will be a function of the potential gradient acting on fluid within the saturated tip. The product of volumetric input and V_g provides a first order measure of the total driving force in a particular slug experiment. Scaled data are shown in Figure 6; average velocities from Table 2 are displayed as open circles. The data appear to indicate that there is a functional relationship between scaled volumetric input and average finger velocity.

Raw data for individual finger width are shown in Figure 7. These data indicate that finger width increases with volumetric input, as suggested by Figure 4. The relationship between width and V_g is somewhat more nebulous, as there appears to be no consistent trend in the data measured at low

volumetric input. This impression is reinforced by the images in Figure 3.

Assuming that volumetric input times V_g provides a measure of forces acting on the fluid within an individual finger, one would expect finger width to display a functional relationship with scaled volumetric input, as does velocity. This relationship is shown as Figure 8; average values again are displayed as open circles. The data suggest that a minimum finger width exists. This result is expected from analogy to Hele-Shaw theory, which predicts a minimum width based on fluid properties, front velocity, and fracture hydraulic properties.

FULL FIELD INSTABILITY: INITIALLY WET FRACTURE

Several experiments investigating gravity-driven wetting front instability in a partially saturated fracture were conducted (see Table 2). These experiments explore two areas: spatial persistence of finger development and effects of a uniform moisture field at field capacity on stability. Fluid was applied to the fracture as a finite slug, distributed from multiple point sources.

Spatial persistence was tested in the full field experiments by applying fluid to a fracture previously wetted by an unstable front and allowed to drain (Figure 9a). Observed behavior appeared to be dependent on the relative volume of the two infiltration events. When volumes were approximately equal, the second wetting front very closely followed the wetted structure of the first event (Figure 9b-d). This persistence is similar to that found in sands by Glass et al.¹⁹ However, unlike observations in sand, the second front was observed to break-up into longer, narrower, more numerous fingers within the pre-

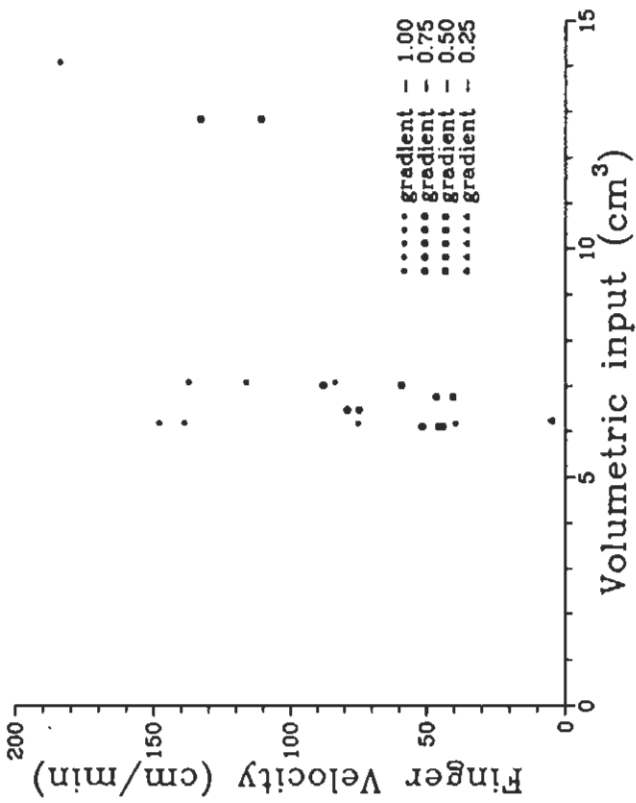


Fig. 5: Raw velocity data from initially dry fractures

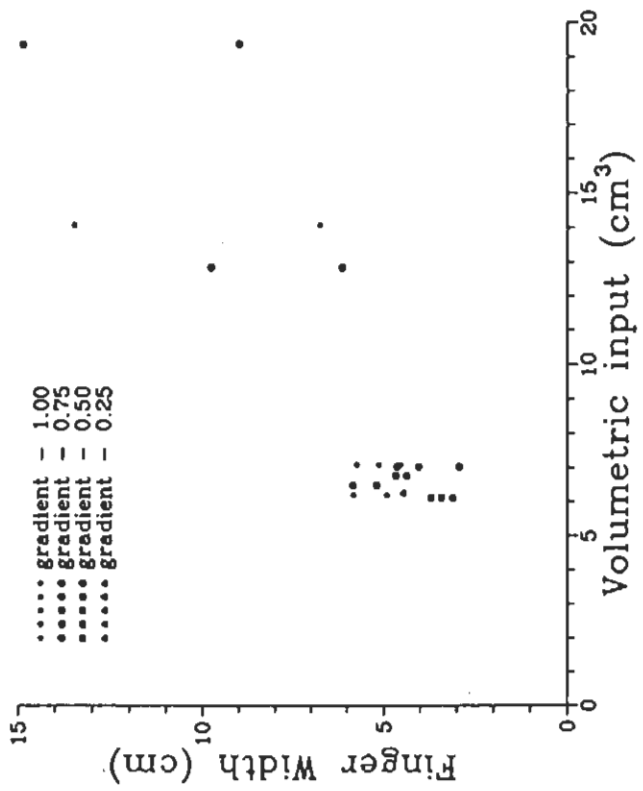


Fig. 7: Raw width data from initially dry fractures

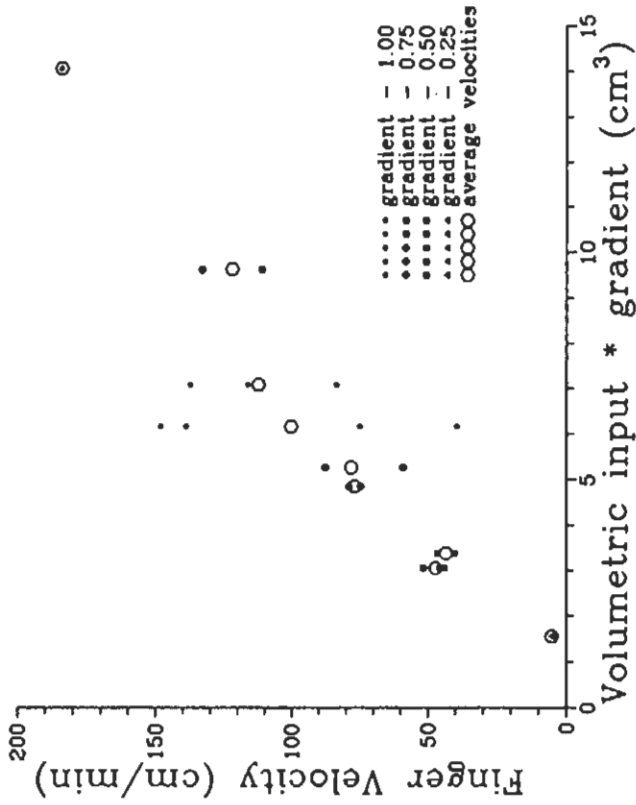


Fig. 6: Scaled velocity data

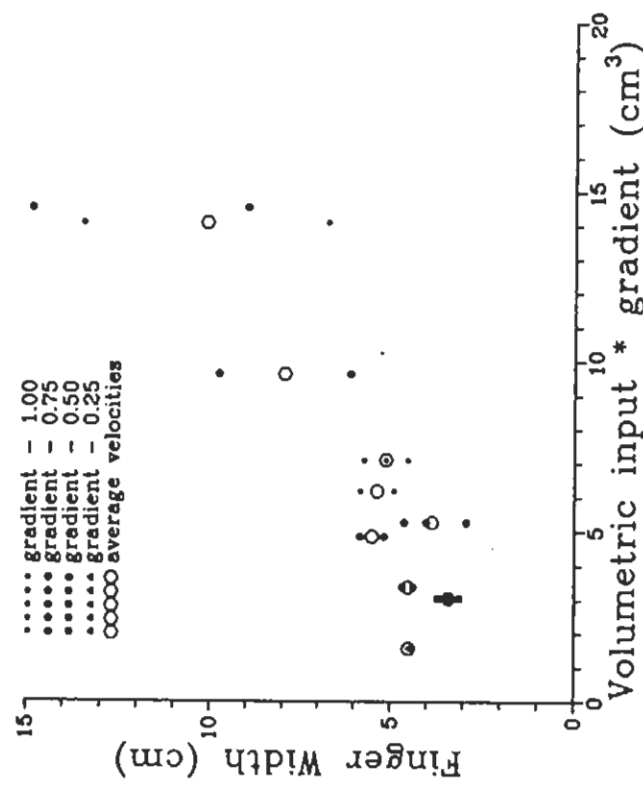


Fig. 8: Scaled width data

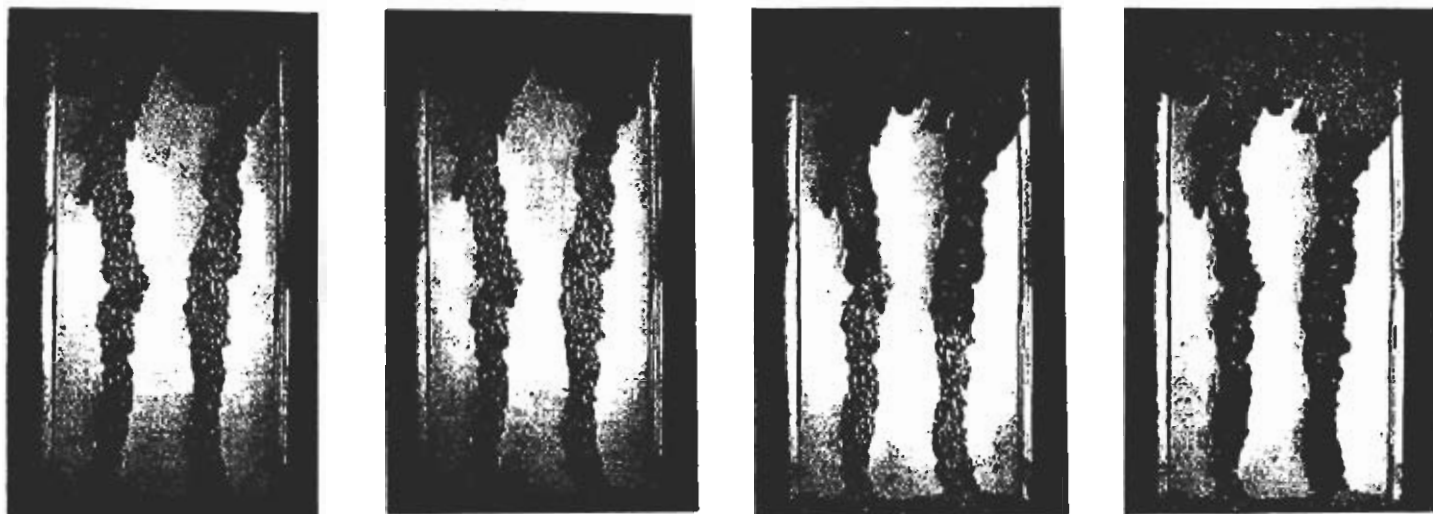


Fig. 9: Sequence illustrating persistence in a prewettered fracture (Experiment 3-1): a) Initial wetted structure left by Experiment 2, b) Stable wetting front, note air entrapment, c) and d) Unstable advancement, note development of sub-fingers in the left structure.

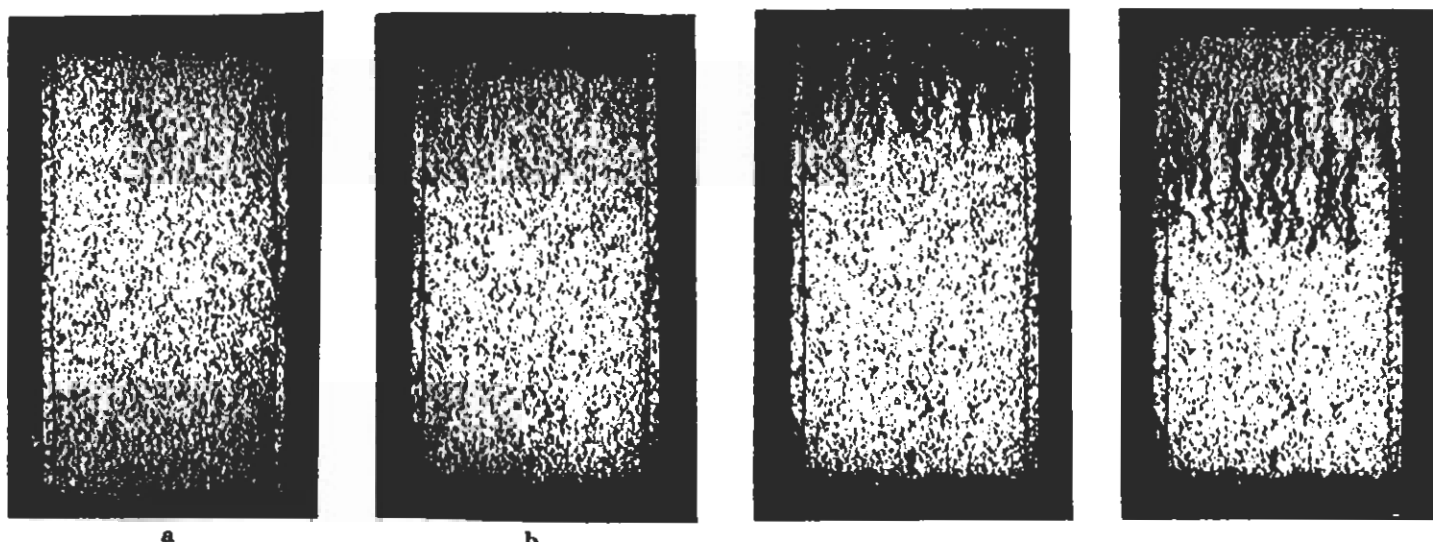


Fig. 10: Sequence illustrating behavior in a uniform wetted structure (Experiment 14): a) Initial uniform wetted structure, b) Stable front imbibition, note complication of the front, c) Onset of instability, note aspect ratio of individual fingers, d) Finger advancement, note consolidation/splitting effects.

wetted structure (Figure 9c). This behavior was accentuated when the second wetting front contained less volume than the first. Again, fingers remained preferentially within the pre-wetted zone. When the second event contained a larger volume than the first there was no change in the number of fingers observed. These fingers preferentially followed the original structure, appearing to overwhelm and widen the individual fingers.

In all cases, the secondary front was observed to be less coherent than the initial wetting front. The structure of the saturated zone was more complicated, containing more entrapped air and extending over a larger domain in the direction

of gravitational gradient. Preliminary observations imply that initial wetted structure will have significant effects on the dynamics of subsequent infiltration events.

To explore the influence of a uniform moisture field, the fracture was filled to saturation, then allowed to drain. With the exception of a capillary fringe along the bottom boundary, this drainage to field capacity produced a relatively homogeneous moisture field (Figure 10a). The stable imbibition front formed after injection of a finite slug (Figure 10b) is found to be much more complicated than those observed in initially dry fractures. Fingers in the unstable front (Figures 10c,d) appear to be more numerous and to

have a higher aspect ratio (length/width) than those observed in initially dry fractures. Individual fingers were observed to wander significantly through the locally heterogeneous hydraulic conductivity field created by the pre-wetted moisture structure, occasionally making abrupt directional changes. Fingers also were noted to split and re-combine more frequently than observed in initially dry fractures; this effect may be an artifact of the small spatial separation between adjacent fingers.

When a prewetted region is contacted by an infiltrating front/finger, the down-gradient edge of the prewetted region immediately becomes the leading edge of the front/finger. This results in a localized step-function increase in L_s and hence V_t . This instantaneous perturbation has a wavelength equivalent to the width of the prewetted region. If these regions are contacted frequently during advancement, finger width will tend towards the predominate width of prewetted regions within the fracture. This behavior differs significantly from that reported for uniformly wetted, partially saturated sands.^{8,20} Under identical flux conditions, fingers were observed to be wider in partially saturated sands than in initially dry sands. Glass et al.²⁰ hypothesized that increased width resulted from an increase in the V_c/V_g ratio due to air entrapment in large pores. This contrasts with the apparent channelization observed in partially saturated fractures.

CONCLUSIONS AND FUTURE DIRECTIONS

We have introduced a systematic approach to investigate the dynamics of wetting front advancement through an unsaturated analog fracture. Preliminary results demonstrate that gravity-driven wetting-front instability occurs in unsaturated rough-walled fractures. The velocity and width of individual fingers depends on inclination of the fracture and volume of fluid within the front/finger. Spatial distribution and relative magnitude of individual fingers appear to be correlated to the distribution and magnitude of finite-amplitude perturbations to the wetting front at the onset of instability.

Observed behavior indicates that wetting-front instability is a persistent and perhaps ubiquitous phenomena that should be considered in modeling unsaturated fracture flow. Validation experiments run over relatively short time spans are likely to encounter wetting-front instability. As such, modeling efforts associated with these studies must account for the effects of instability on inter-block connectivity, wetting-front velocity, effective wetted domain, and transport properties.

Gravity-driven wetting-front instability has numerous implications with regard to modeling of unsaturated fracture flow; consider one simple

scenario. A low-permeability rock unit containing extensive, non-horizontal, unsaturated fractures outcrops at the surface. On cessation of imbibition into the fractures after an intense rainfall event, the advancing front within the fractures becomes unstable. Fingers transport water and solutes downward until the advancing saturated tips are depleted of water left behind on the fracture walls. A subsequent rainstorm occurs in a timeframe short with respect to matrix imbibition so that water now moves through the prewetted fracture directly to the stalled fingertips from the previous event and the fingers resume growth, now with the entire volume of water supplied from the second precipitation event. Such a combination of rainstorms promotes rapid recharge and transport of solutes through a fractured formation.

The preliminary experiments presented here are part of an ongoing research program. The limited data set (Table 2) is in the process of being completed. In initially dry fractures, at each V_g the range of potential flow volumes is being explored. Experiments are being performed to discover the value of L_s corresponding to "freezing" of the front and the maximum volume allowing finger development as a function of fracture length, and to delineate intermediate behavior. Similar experiments are being performed in pre-wetted fractures. We are also in the process of further analyzing the data already collected.

Current work in progress also includes investigation of the behavior of single fingers. Initiating a finger from a single point source allows systematic variation of flux into the finger. It is expected that relationships describing finger width and velocity as functions of q , V_g , and system parameters can be developed. Concentrating on a single finger allows increased spatial resolution and hence, detailed characterization of the wetted structure, including calculation of the fractal dimension for the interface. Aperture-scale models capable of predicting finger structure in the quasistatic limit are undergoing concurrent development.²¹

Preparations are underway to investigate the effect of aperture structure on gravity-driven wetting-front stability. Three experimental approaches are being developed concurrently. The aperture structure of the simple fracture described in this paper will be varied by using plates with different topographies in combination with flat fracture plates. Addition of length scales will be accomplished by sandblasting the plates. This addition of micro-roughness is expected to induce significant film flow. Plans also include direct manufacture of glass plates with a predetermined aperture field. Graphite blocks, precision machined on a numerically controlled milling machine will be used to cast the fracture aperture. The aperture distribution can be controlled completely within the tolerance

limits of the milling process. Finally, plans are underway to perform experiments in both natural fractures and in epoxy casts of fracture surfaces.

ACKNOWLEDGEMENTS

The authors gratefully acknowledge the assistance and support of W.C. Ginn in design and fabrication of the experimental apparatus, L. Orear in development of image acquisition software, and V. McConnell in development of experimental procedure and conduct of several scoping experiments. This work was supported by the U.S. Department of Energy, Office of Civilian Radioactive Waste Management, Yucca Mountain Site Characterization Project Office, under contract DE-AC04-76DP00789.

REFERENCES

1. R.J. GLASS, "Laboratory Research Program to Aid in Developing and Testing the Validity of Conceptual Models for Flow and Transport Through Unsaturated Porous Media", Proceedings of the Geoval-90 Symposium, May 14-20, 1990, Stockholm, Sweden, 275-283 (1990).
2. R.J. GLASS and V.C. TIDWELL, "Research Program to Develop and Validate Conceptual Models for Flow and Transport Through Unsaturated, Fractured Rock", Proc. of the Sec. Annual Int. Conf. on High Level Radioactive Waste Management, April 28-May 3, 1991, Las Vegas, Nevada, 977-987 (1991).
3. I. WINOGRAD, "Radioactive Waste Disposal in Thick Unsaturated Zones", Science, 212, 1457-1464 (1981).
4. R.W. BARNARD and H.A. DOCKERY, "Yucca Mountain Project Total-System Performance Assessment Preliminary Analysis: Overview", Proc. of the Third Annual Int. Conf. on High Level Radioactive Waste, Las Vegas, Nevada, April 12-16 (1992).
5. R.J. GLASS and D.L. NORTON, "Wetted Region Structure in Horizontal Unsaturated Fractures: Water Entry Through the Surrounding Porous Matrix", Proc. of the Third Annual Int. Conf. on High Level Radioactive Waste, Las Vegas, Nevada, April 12-16 (1992).
6. D.E. HILL and J.-Y. PARLANGE, "Wetting Front Instability in Layered Soils", Soil Sci. Soc. Am. Proc., 36, 697-702 (1972).
7. G.A. DIMENT and K.K. WATSON, "Stability Analysis of Water Movement in Unsaturated Porous Materials 3. Experimental Studies", Water Resour. Res., 21, 979-984 (1985).
8. R.J. GLASS, J.-Y. PARLANGE and T.S. STEENHUIS, "Wetting Front Instability I: Theoretical Discussion and Dimensional Analysis", Water Resour. Res., 25, 1187-1194 (1989).
9. R.J. GLASS, T.S. STEENHUIS and J.-Y. PARLANGE, "Wetting Front Instability II: Experimental Determination of Relationships Between System Parameters and Two-Dimensional Unstable Flow Field Behavior in Initially Dry Porous Media", Water Resour. Res., 25, 1195-1207 (1989).
10. R.J. GLASS, J.-Y. PARLANGE and T.S. STEENHUIS, "Immiscible Displacement in Porous Media: Stability Analysis of Three-Dimensional, Axisymmetric Disturbances with Application to Gravity-Driven Wetting Front Instability", Water Resour. Res., 27, 1947-1956 (1991).
11. P.G. SAFFMAN and G. TAYLOR, "The Penetration of a Fluid Into a Porous Medium or Hele-Shaw Cell Containing a More Viscous Liquid", Proc. Roy. Soc. London, A245, 312-331 (1958).
12. R.L. CHOUKE, P. VAN MEURS, and C. VAN DER POEL, "The Instability of Slow Immiscible, Viscous Liquid-Liquid Displacements in Porous Media", Trans. Am. Inst. Min. Eng., 216, T.P. 8073 (1959).
13. P.G. SAFFMAN, "Viscous Fingering in Hele-Shaw Cells", J. Fl. Mech., 173, 73 (1986).
14. G.M. HOMS, "Viscous Fingering in Porous Media", Ann. Rev. Fluid Mech., 19, 271-311 (1987).
15. T. MAXWORTHY, "The Nonlinear Growth of a Gravitationally Unstable Interface in a Hele-Shaw Cell", J. Fl. Mech., 177, 207-232 (1987).
16. J.-Y. PARLANGE and D.E. HILL, "Theoretical Analysis of Wetting Front Instability in Soils", Soil Sci., 122, 236-239 (1976).
17. R.J. GLASS, M.J. NICHOLL, and M.E. THOMPSON, "Comparison of Measured and Calculated Permeability for a Saturated, Rough-Walled Fracture", Presented at the Fall 1991 AGU Meeting, (H51D-11) EOS, 72, 216 (1991).
18. D. WILKINSON and J.F. WILLEMSSEN, "Invasion Percolation: A New Form of Percolation Theory", J. Phys. A: Math. Gen., 16, 3365-3376 (1983).
19. R.J. GLASS, T.S. STEENHUIS, and J.-Y. PARLANGE, "Mechanism for Finger Persistence in Homogeneous Unsaturated Porous Media: Theory and Verification", Soil Sci., 148, 60-70 (1989).
20. R.J. GLASS, J.-Y. PARLANGE and T. STEENHUIS, "Water infiltration in layered soils where a fine textured layer overlays a coarse sand," Proc. of the Int. Conf. for Infiltration Devel. and App., Hawaii, Jan 5-9, 1987, 66-81 (1987).
21. R.J. GLASS and L. YARRINGTON, "Analysis of Wetting Front Instability Using Modified Invasion Percolation Theory," Presented at the Fall 1989 AGU Meeting, (H42D-02) EOS, 70, 43, 1117 (1989).